Computers and Concrete, *Vol. 25, No. 4* (*2020*) *311-325*
DOI: https://doi.org/10.12989/cac.2020.25.4.311

Effects of hygro-thermo-mechanical conditions on the buckling of FG sandwich plates resting on elastic foundations

Salah Refrafi[1,2], Abdelmoumen Anis Bousahla[3,4], Abdelhakim Bouhadra[1,2], Abderrahmane Menasria[1,2], Fouad Bourada[1,5], Abdeldjebbar Tounsi[1], E.A. Adda Bedia[4], S.R. Mahmoud[6], Kouider Halim Benrahou[1] and Abdelouahed Tounsi*[1,4]

[1] *Materials and Hydrology Laboratory, University of Sidi Bel Abbes, Faculty of Technology, Civil Engineering Department, Algeria*
[2] *Civil Engineering Department, Faculty of Science &Technology, Abbes Laghrour University, Khenchela, Algeria*
[3] *Laboratoire de Modélisation et Simulation Multi-échelle, Université de Sidi Bel Abbés, Algeria*
[4] *Department of Civil and Environmental Engineering, King Fahd University of Petroleum & Minerals, 31261 Dhahran, Eastern Province, Saudi Arabia.*
[5] *Département des Sciences et de la Technologie, centre universitaire de Tissemsilt, BP 38004 Ben Hamouda, Algeria*
[6] *GRC Department, Jeddah Community College, King Abdulaziz University, Jeddah, Saudi Arabia*

(*Received January 6, 2020, Revised March 13, 2020, Accepted March 14, 2020*)

Abstract. In this research work, the hygrothermal and mechanical buckling responses of simply supported FG sandwich plate seated on Winkler-Pasternak elastic foundation are investigated using a novel shear deformation theory. The current model take into consideration the shear deformation effects and ensures the zero shear stresses on the free surfaces of the FG-sandwich plate without requiring the correction factors "*Ks*". The material properties of the faces sheets of the FG-sandwich plate are assumed varies as power law function "P-FGM" and the core is isotropic (purely ceramic). From the virtual work principle, the stability equations are deduced and resolved via Navier model. The hygrothermal effects are considered varies as a nonlinear, linear and uniform distribution across the thickness of the FG-sandwich plate. To check and confirm the accuracy of the current model, a several comparison has been made with other models found in the literature. The effects the temperature, moisture concentration, parameters of elastic foundation, side-to-thickness ratio, aspect ratio and the inhomogeneity parameter on the critical buckling of FG sandwich plates are also investigated.

Keywords: buckling; hygrothermal effect; elastic foundation; Hamilton's principle; Navier solution

1. Introduction

The sandwich plates are a structural element composed of two faces sheet and one core (Thai *et al*. 2014, Borsellino *et al*. 2004). Because of its low weight and high rigidity, this type of structure element has been widely employed in several sectors such as construction, aerospace, transport, aeronautic and marine and others engineering (Wang *et al*. 2010, Yeh 2013, Chakrabarti and Sheikh 2005, Pandit *et al*. 2008, Kant and Swaminathan 2002, Nayak *et al*. 2002, Mantari *et al*. 2012, Mehar *et al*. 2019, Rajabi and Mohammadimehr 2019).The three elements of the classical composite sandwich plates are adhesively bonded which increases the delamination risk. To avoid this problem, Japanese researches laboratories have created the new class of materials called FGMs which eliminate the interfaces areas that represents an area of accumulation and concentrations of stresses. Several researchers used this this kind of materials in the FG-sandwich structure (Li *et al*. 2008, Liu and Jeffers 2017, Xiang *et al*. 2011). For studying the various behaviors of the thick FG-sandwich plate, many analytical models are proposed.

Kiani and Eslami (2011) studied the stability of the porous FG-sandwich plate under thermal load using the first-shear deformation theory (FSDT). Mantari and Granados (2015) proposed a novel first shear deformation model based on the undetermined integral for studying the flexural analysis of the FG-sandwich plate with an FG core and isotropic skins. Sobhy (2013) investigated on the stability and dynamic behavior of the EFG-sandwich plates with various types of support using five variables shear deformation theory. Nguyen *et al*. (2014) developed an inverse-tangential higher-order shear-deformation theory for studying the bending, buckling and free-vibrational behaviors of the FG-sandwich plate with isotropic core and FG-faces sheets and FG-sandwich plate with FG-core and isotropic faces sheets. Based on HSDT theory, Natarajan and Manickam (2012) investigated on static and dynamic behaviors of the FG-sandwich plate using 8-noded quadrilateral plate element. Akavci (2016) developed a new hyperbolic warping function shape for the analyze of the various behaviors of the FG-sandwich plate seated on Winkler-Pasternak elastic foundation. Using the layerwise FE formulation based on the FSDT assumption, Pandey and Pradyumna (2015) have examined the free vibration of the FG-sandwich plate. The Natural frequencies of the rectangular sandwich plate with FG-face and homogeneous core has been computed by Xiang *et al*. (2011) by

*Corresponding author, Professor
E-mail: tou_abdel@yahoo.com

http://www.techno-press.org/?journal=cac&subpage=8 ISSN: 1598-8198 (Print), 1598-818X (Online)

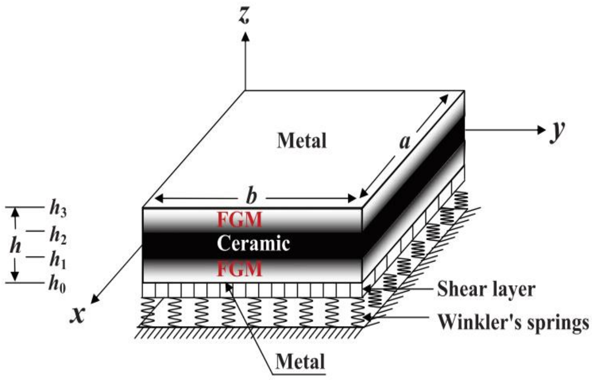

Fig. 1 Geometry of the FGM sandwich plate

employing the nth-order shear deformation theory. Iurlaro *et al*. (2014) has extended the refined zigzag theory for examining the static and dynamic analysis of the FG-sandwich plates. Recently, several research work on sandwich plate are published such as (Raissi *et al*. 2018, Rezaiee-Pajand *et al*. 2018, Tomar and Talha 2018, Lieu *et al*. 2018, Singh and Harsha 2018, Akbas 2019a, Burlayenko and Sadowski 2019, Emdadi *et al*. 2019, Rezaiee-Pajand *et al*. 2019, Heshmati and Jalali 2019, Beni 2019, Mirjavadi *et al*. 2019b, Hamed *et al*. 2020, Eltaher and Mohamed 2020).

The purpose of this work is to proposing a novel four unknowns hyperbolic-HSDT to examine the non-linear hygrothermal and mechanical stability of the simply supported FG-sandwich plate on elastic foundation type "Winkler-Pasternak". The transverse shear effect is considered without any correction. The equilibrium equations and analytical solution of the hygrothermal and mechanical-buckling of the FG-sandwich plate are derived via virtual work principle and Navier model, respectively. Moreover, the efficiency an accuracy of the current theory is confirmed by comparing the computed results with published ones. Thereafter, several parametric studies are presented and discussed in detail.

2. Mathematical formulation

Let us consider an FG-sandwich plate of thickness "h", length "a" and width "b" composed of three layers (metal-ceramic, ceramic, and ceramic-metal) as shown in Fig. 1. The top and bottom faces-sheets of the plate are at $z=\pm h/2$. The vertical positions of the top, bottom and the two interfaces between the layers are denoted by $h_0=-h/2$, $h_3=h/2$, h_1 and h_2, respectively. The FG-sandwich-plate is assumed to be surrounded by the elastic-foundation.

The effective material properties for each layer, such as thermal conductivity "K", Young's modulus "E", Poisson's ratio "v", coefficient of thermal-expansion "α" and coefficient of moisture -expansion "β", are assumed to be determined as (Zenkour and Sobhy 2010, Radwan 2017, Ebrahimi and Barati 2017a, b, Akbas 2019b, Hadji *et al*. 2019, Sahouane *et al*. 2019)

$$\begin{gathered} P^{(j)}(z) = (P_c - P_m)V^{(j)}(z) + P_m \\ P = E, \beta, \alpha, K \end{gathered} \tag{1}$$

Where "$V^{(j)}$" is the volume fraction of j-layer and can be expressed as

$$\begin{cases} V^{(1)}(z) = \left(\dfrac{z-h_0}{h_1-h_0}\right)^k & \text{for } z \in [h_0, h_1] \\ V^{(2)}(z) = 1 & \text{for } z \in [h_1, h_2] \\ V^{(3)}(z) = \left(\dfrac{z-h_3}{h_2-h_3}\right)^k & \text{for } z \in [h_2, h_3] \end{cases} \tag{2}$$

where the subscripts m and c denote the metallic and ceramic components, respectively. in the case of k equal to zero indicates a fully ceramic-plate, whereas $k=\infty$ represents a fully metallic-plate.

The plate is assumed to seat on two-parameter elastic-foundation model which consists of closely spaced springs interconnected through a shear-layer made of incompressible vertical elements, which deform only by transverse shear. The response equation "R_f" of this foundation is given by

$$R_f = K_w w - K_p \nabla^2 w \tag{3}$$

Where "K_w" and "K_p" are spring (Winkler) and shear (Pasternak) foundation stiffnesses, respectively.

2.1 Kinematics and strains

In this work, the classical HSDT is modified by considering some simplifying assumptions in which to reduce the unknowns-number. The displacement field formulation of the conventional HSDT is given by

$$\begin{gathered} u(x,y,z) = u_0(x,y) - z\frac{\partial w_0}{\partial x} + f(z)\phi_x(x,y) \\ v(x,y,z) = v_0(x,y) - z\frac{\partial w_0}{\partial y} + f(z)\phi_y(x,y) \\ w(x,y,z) = w_0(x,y) \end{gathered} \tag{4}$$

u_0, v_0, w_0, Φx and Φy are the five-unknown displacements of the mid-plane of the plate. By considering that $\phi_x = \int \theta(x,y)dx$ and $\phi_y = \int \theta(x,y)dy$. The displacement fields mentioned above can be rewritten as follows

$$\begin{gathered} u(x,y,z) = u_0(x,y) - z\frac{\partial w_0}{\partial x} + k_1 f(z)\int \theta(x,y)\,dx \\ v(x,y,z) = v_0(x,y) - z\frac{\partial w_0}{\partial y} + k_2 f(z)\int \theta(x,y)\,dy \\ w(x,y,z) = w_0(x,y) \end{gathered} \tag{5}$$

In the present study, the shape function is proposed in hyperbolic form as

$$f(z) = (0.1212\pi z)\left[\pi - (0.135)^{1/3}\cosh\left(\frac{\pi z}{h}\right)\right] \tag{6}$$

The transverse shear strain function is an even function which is the 1st derivation of the shape function ($g(z)=f'(z)$). Therefore, the current shear shape-function satisfies the zero-stresses at top and bottom surfaces of the plate.

$$\begin{gathered} \begin{Bmatrix} \varepsilon_x \\ \varepsilon_y \\ \gamma_{xy} \end{Bmatrix} = \begin{Bmatrix} \varepsilon_x^0 \\ \varepsilon_y^0 \\ \gamma_{xy}^0 \end{Bmatrix} + z\begin{Bmatrix} k_x^b \\ k_y^b \\ k_{xy}^b \end{Bmatrix} + f(z)\begin{Bmatrix} k_x^s \\ k_y^s \\ k_{xy}^s \end{Bmatrix}, \begin{Bmatrix} \gamma_{yz} \\ \gamma_{xz} \end{Bmatrix} = \\ g(z)\begin{Bmatrix} \gamma_{yz}^0 \\ \gamma_{xz}^0 \end{Bmatrix} \end{gathered} \tag{7}$$

Where

$$\begin{Bmatrix} \varepsilon_x^0 \\ \varepsilon_y^0 \\ \gamma_{xy}^0 \end{Bmatrix} = \begin{Bmatrix} \frac{\partial u_0}{\partial x} \\ \frac{\partial v_0}{\partial y} \\ \frac{\partial u_0}{\partial y} + \frac{\partial v_0}{\partial x} \end{Bmatrix}, \quad \begin{Bmatrix} k_x^b \\ k_y^b \\ k_{xy}^b \end{Bmatrix} = \begin{Bmatrix} -\frac{\partial^2 w_0}{\partial x^2} \\ -\frac{\partial^2 w_0}{\partial y^2} \\ -2\frac{\partial^2 w_0}{\partial x \partial y} \end{Bmatrix}, \tag{8a}$$

$$\begin{Bmatrix} k_x^s \\ k_y^s \\ k_{xy}^s \end{Bmatrix} = \begin{Bmatrix} k_1 \theta \\ k_2 \theta \\ k_1 \frac{\partial}{\partial y} \int \theta dx + k_2 \frac{\partial}{\partial x} \int \theta dy \end{Bmatrix}, \quad \begin{Bmatrix} \gamma_{yz}^0 \\ \gamma_{xz}^0 \end{Bmatrix} = \begin{Bmatrix} k_2 \int \theta dy \\ k_1 \int \theta dx \end{Bmatrix}, \tag{8b}$$

The integrals " $\int \theta\, dx$" and " $\int \theta\, dy$" used in the above Eqs. (5) and (8b) shall be resolved by a Navier-procedure and can be given as follows

$$\frac{\partial}{\partial y} \int \theta\, dx = A' \frac{\partial^2 \theta}{\partial x \partial y}, \quad \frac{\partial}{\partial x} \int \theta\, dy = B' \frac{\partial^2 \theta}{\partial x \partial y}, \quad \int \theta\, dx = A' \frac{\partial \theta}{\partial x}, \quad \int \theta\, dy = B' \frac{\partial \theta}{\partial y} \tag{9a}$$

Where the coefficients "A'" and "B'" are expressed according to the type of solution used, in this case is Navier method. Therefore, "A', B', k_1 and k_2" are expressed as follows

$$A' = -\frac{1}{\mu^2}, B' = -\frac{1}{\beta^2}, k_1 = \mu^2, k_2 = \beta^2 \tag{9b}$$

Where "μ and β" are used in expression (30).

It should be noted that unlike the FSDT, this current model does not require shear correction coefficients.

2.2 Constitutive relations

The stresses-strains relations of the FG-plate can be expressed as

$$\begin{Bmatrix} \sigma_x \\ \sigma_y \\ \tau_{yz} \\ \tau_{xz} \\ \tau_{xy} \end{Bmatrix}^{(j)} = \begin{bmatrix} C_{11} & C_{12} & 0 & 0 & 0 \\ C_{12} & C_{22} & 0 & 0 & 0 \\ 0 & 0 & C_{44} & 0 & 0 \\ 0 & 0 & 0 & C_{55} & 0 \\ 0 & 0 & 0 & 0 & C_{66} \end{bmatrix}^{(j)} \begin{Bmatrix} \varepsilon_x - \alpha T - \beta C \\ \varepsilon_y - \alpha T - \beta C \\ \gamma_{xy} \\ \gamma_{yz} \\ \gamma_{xz} \end{Bmatrix}^{(j)} \tag{10}$$

where "C_{ij} (i,j=1,2,3,4,5,6)" are the expressions in terms of engineering constants given as

$$C_{11}^{(j)} = C_{22}^{(j)} = \frac{E^{(j)}(z)}{1-\nu^2}, C_{12}^{(j)} = \frac{\nu E^{(j)}(z)}{1-\nu^2}, \quad C_{44}^{(j)} = C_{55}^{(j)} = C_{66}^{(j)} = \frac{E^{(j)}(z)}{2(1+\nu)}, \tag{11}$$

2.3 The stability equations

The virtual-work principle for the FG sandwich-plate resting on elastic foundations under biaxial compression load can be expressed as (Zouatnia *et al.* 2019)

$$\begin{aligned} \int_A [& N_x \delta\varepsilon_x^0 + N_y \delta\varepsilon_y^0 + N_{xy}\delta\gamma_{xy}^0 + M_x^b \delta k_x^b + M_y^b \delta k_y^b \\ & + M_{xy}^b \delta k_{xy}^b + M_x^s \delta k_x^s + M_y^s \delta k_y^s + M_{xy}^s \delta k_{xy}^s + S_{yz}^S \delta\gamma_{yz} \\ & + S_{xz}^S \delta\gamma_{xz} + \left(\bar{R}_f - \frac{N_x}{b}\frac{\partial^2 w}{\partial x^2} - \frac{N_y}{a}\frac{\partial^2 w}{\partial y^2} \right) \delta w] dA = 0 \end{aligned} \tag{12}$$

where, the stress and moment resultants are defined by

$$(N_i, M_i^b, M_i^s) = \sum_{j=1}^{3} \int_{h_{j-1}}^{h_j} (1, z, f) \sigma_i^{(j)} dz \;, (i = x, y, xy) \tag{13a}$$

And

$$(S_{xz}^s, S_{yz}^s) = \sum_{j=1}^{3} \int_{h_{j-1}}^{h_j} g(\tau_{xz}, \tau_{yz})^{(j)} dz \tag{13b}$$

Substituting the Eq. (7) into Eq. (10) and the subsequent results into Eq. (13) the stress and moment resultants are obtained in the matrix form as

$$\begin{Bmatrix} N_x \\ N_y \\ N_{xy} \\ M_x^b \\ M_y^b \\ M_{xy}^b \\ M_x^s \\ M_y^s \\ M_{xy}^s \end{Bmatrix} = \begin{bmatrix} A_{11} & A_{12} & 0 & B_{11} & B_{12} & 0 & B_{11}^s & B_{12}^s & 0 \\ A_{12} & A_{22} & 0 & B_{12} & B_{22} & 0 & B_{12}^s & B_{22}^s & 0 \\ 0 & 0 & A_{66} & 0 & 0 & B_{66} & 0 & 0 & B_{66}^s \\ B_{11} & B_{12} & 0 & D_{11} & D_{12} & 0 & D_{11}^s & D_{12}^s & 0 \\ B_{12} & B_{22} & 0 & D_{12} & D_{22} & 0 & D_{12}^s & D_{22}^s & 0 \\ 0 & 0 & B_{66} & 0 & 0 & D_{66} & 0 & 0 & D_{66}^s \\ B_{11}^s & B_{12}^s & 0 & D_{11}^s & D_{12}^s & 0 & H_{11}^s & H_{12}^s & 0 \\ B_{12}^s & B_{22}^s & 0 & D_{12}^s & D_{22}^s & 0 & H_{12}^s & H_{22}^s & 0 \\ 0 & 0 & B_{66}^s & 0 & 0 & D_{66}^s & 0 & 0 & H_{66}^s \end{bmatrix} \begin{Bmatrix} \varepsilon_x^0 \\ \varepsilon_y^0 \\ \gamma_{xy}^0 \\ k_x^b \\ k_y^b \\ k_{xy}^b \\ k_x^s \\ k_y^s \\ k_{xy}^s \end{Bmatrix} - \begin{Bmatrix} N_x^T \\ N_y^T \\ 0 \\ M_x^{bT} \\ M_y^{bT} \\ 0 \\ M_x^{sT} \\ M_y^{sT} \\ 0 \end{Bmatrix} - \begin{Bmatrix} N_x^C \\ N_y^C \\ 0 \\ M_x^{bC} \\ M_y^{bC} \\ 0 \\ M_x^{sC} \\ M_y^{sC} \\ 0 \end{Bmatrix} \tag{14a}$$

$$\begin{Bmatrix} S_{yz}^s \\ S_{xz}^s \end{Bmatrix} = \begin{bmatrix} A_{44}^s & 0 \\ 0 & A_{55}^s \end{bmatrix} \begin{Bmatrix} \gamma_{yz}^0 \\ \gamma_{xz}^0 \end{Bmatrix} \tag{14b}$$

where $A_{11}, B_{11}\ etc.$ stiffness components are expressed as

$$\begin{Bmatrix} A_{11} & B_{11} & D_{11} & B_{11}^s & D_{11}^s & H_{11}^s \\ A_{12} & B_{12} & D_{12} & B_{12}^s & D_{12}^s & H_{12}^s \\ A_{66} & B_{66} & D_{66} & B_{66}^s & D_{66}^s & H_{66}^s \end{Bmatrix} = \sum_{j=1}^{3} \int_{h_{j-1}}^{h_j} C_{11}^{(j)} (1, z, z^2, f(z), z\, f(z), f^2(z)) \begin{Bmatrix} 1 \\ \nu \\ \frac{1-\nu}{2} \end{Bmatrix} dz$$

$$(A_{22}, B_{22}, D_{22}, B_{22}^s, D_{22}^s, H_{22}^s) = (A_{11}, B_{11}, D_{11}, B_{11}^s, D_{11}^s, H_{11}^s)$$

$$A_{44}^s = A_{55}^s = \sum_{j=1}^{3} \int_{h_{j-1}}^{h_j} C_{44}^{(j)} \left[g(z)\right]^2 dz, \tag{14c}$$

The stress and moment resultants $N_x^\Theta = N_y^\Theta$; $M_x^{b\Theta} = M_y^{b\Theta}$ and $M_x^{s\Theta} = M_y^{s\Theta}$; (Θ=T,C) due to hygrothermal-loading are defined as

$$\begin{Bmatrix} N_x^\Theta \\ M_x^{b\Theta} \\ M_y^{b\Theta} \end{Bmatrix} = \sum_{j=1}^{3} \int_{h_{j-1}}^{h_j} \frac{E^{(j)}(z)}{1-\nu} \Upsilon^{(j)}(z)\Theta(z) \begin{Bmatrix} 1 \\ z \\ f(z) \end{Bmatrix} dz \tag{16}$$

Where

$$\Theta(z) = \begin{cases} C(z) & if \ \Upsilon = \beta \\ T(z) & if \ \Upsilon = \alpha \end{cases} \tag{17}$$

Supposing the displacement terms u_0^0; v_0^0; w_0^0 et θ^0 the equilibrium-state of the FG sandwich plate under hygrothermal-loads. Let the terms of displacements u_0^1; v_0^1; w_0^1 et θ^1 are a neighboring stable-state with respect to the equilibrium position. Therefore, the general displacements of a neighboring state (Radwan 2017) are

$$\begin{aligned} u_0 = u_0^0 + u_0^1 \quad , \quad v_0 = v_0^0 + v_0^1 \quad , \\ w_0 = w_0^0 + w_0^1 \quad , \quad \theta_0 = \theta^0 + \theta^1 \end{aligned} \tag{18}$$

Wherethe superscript 0 and 1 indicates the state of equilibrium conditions and the state of stability, respectively. By collecting the coefficients u_0^1; v_0^1; w_0^1 et θ^1 in the virtual work (Eq. (12)), the stability equations are obtained as

$$\begin{gathered} \frac{\partial N_x^1}{\partial x} + \frac{\partial N_{xy}^1}{\partial y} = 0 \\ \frac{\partial N_{xy}^1}{\partial x} + \frac{\partial N_y^1}{\partial y} = 0 \\ \frac{\partial^2 M_x^{b1}}{\partial x^2} + 2\frac{\partial^2 M_{xy}^{b1}}{\partial x \partial y} + \frac{\partial^2 M_y^{b1}}{\partial y^2} + N_0 - \bar{R}_f = 0 \\ -k_1 M_x^{s1} - k_2 M_y^{s1} - (k_1 A' + k_2 B')\frac{\partial^2 M_{xy}^{s1}}{\partial x \partial y} \\ +k_1 A' \frac{\partial S_{xz}^{s1}}{\partial x} + +k_2 B' \frac{\partial S_{yz}^{s1}}{\partial y} = 0 \end{gathered} \tag{19}$$

Where

$$N_0 = N_x^0 \frac{\partial^2 w_0^1}{\partial x^2} + N_y^0 \frac{\partial^2 w_0^1}{\partial y^2} \tag{20}$$

in which N_x^0 and N_y^0 are given as

$$\begin{gathered} N_x^0 = N_x^M + N_x^H, \quad N_y^0 = N_y^M + N_y^H, \\ N_x^M = -\frac{N_x}{b} \ , \ N_y^M = -\frac{N_y}{a} \ , \ \frac{N_x^M}{N_y^M} = R, \end{gathered} \tag{21a}$$

$$N_x^H = N_y^H = -\sum_{j=1}^{3} \int_{h_{j-1}}^{h_j} \frac{E^{(j)}(z)}{1-\nu} (\alpha^j(z)T(z) \tag{21b}$$

$$+\beta^j(z)C(z))dz \tag{21c}$$

2.4 Various types of hygrothermal rise

In this study, the simply-supported is subjected to three hygrothermal distributions type through the thickness are non-linear, linear and uniform. Each type of the hygrothermal distributions is accurately depicted below.

2.4.1 Uniform hygrothermal rise (UHR)

In the first type, the FG-sandwich plate is subjected to an initial temperature and moisture "T_i" and "C_i", and then the moisture and temperature were uniformly increased to the final values "T_f" and "C_f". with

$$\Delta\Theta = \Theta_f - \Theta_i \quad , \quad \Theta = \mathrm{T,C} \tag{22}$$

2.4.2 Linear hygrothermal rise (LHR)

The second type of the hygrothermal distribution is linear and can be presented in the following form

$$\begin{gathered} \Theta(z) = \Delta\Theta\left(\frac{1}{2} + \frac{z}{h}\right) + \Theta_l \\ \Theta(z) = \Delta\Theta\left(\frac{1}{2} + \frac{z}{h}\right) + \Theta_l \end{gathered} \tag{23}$$

Where "Θ_l and Θ_u" are the hygrothermal at the lower and upper surface of the FG-sandwich plate and $\Delta\Theta = \Theta_u - \Theta_l$.

2.4.3 Non-linear hygrothermal rise (NHR)

In this case, the temperature distribution through-the-thickness has been given according to the following approaches:

1. In the first case, the temperature of the top surface is T_t and it is considered to vary from T_t to Tb in which the plate buckles, according to the power law variation through-the-thickness, to the bottom surface temperature Tb in which the plate buckles. Therefore, the temperature rise through-the-thickness is given by

$$\Theta(z) = \Delta\Theta\left(\frac{1}{2} + \frac{z}{h}\right)^\gamma + \Theta_l \tag{24}$$

where is the hygrothermal exponent, $1 < \gamma < \infty$

2. In the second case, the one-dimensional Fourier equation of thermal conduction, is solved.

$$\begin{cases} \frac{d}{dz}\left[k(z)\frac{dT}{dz}\right] = 0 & -\frac{h}{2} < z < \frac{h}{2} \\ T = T_c & z = \frac{h}{2} \\ T = T_m & z = -\frac{h}{2} \end{cases} \tag{25}$$

$k(z)$ is the coefficient of thermal conduction, T_c and T_m denote the temperature changes at the ceramic side and the metal side, respectively. Similar to the coefficients of elastic moduli and thermal expansion, the coefficient of thermal conduction is also assumed as a power-form of coordinate variable z as

$$k(z) = (k_c - k_m)V_c^k + k_m \tag{26}$$

The Eq. (25) can be solved using a polynomial power-series expansion given as

$$\begin{gathered} T(z) = T_m + \frac{(T_c - T_m)}{L} \\ \left(\frac{z}{h} + \frac{1}{2}\right) \sum_{i=0}^{N_T} \left[(-1)^i \frac{\left(\frac{z}{h} + \frac{1}{2}\right)^{ip} (K_c - K_m)^i}{(ip+1)K_m} \right] \end{gathered} \tag{27}$$

where N_T is the number of series' terms, which in the case of non-uniform temperature rise is obtained from a convergence study. L is defined as follows

$$L = \sum_{i=0}^{N_T} \left[(-1)^i \frac{(K_c - K_m)^i}{(ip+1)K_m} \right] \tag{28}$$

3. Analytical solution

Based on the Navier procedure (Akbas 2017, Safa *et al.* 2019), the following expansions of displacements $\boldsymbol{u_0^1}$; $\boldsymbol{v_0^1}$; $\boldsymbol{w_0^1}$ et $\boldsymbol{\theta^1}$ are chosen to satisfy automatically the boundary conditions of the FG-sandwich plate.

$$\begin{Bmatrix} u_0^1 \\ v_0^1 \\ w_0^1 \\ \theta^1 \end{Bmatrix} = \sum_{m=1}^{\infty} \sum_{n=1}^{\infty} \begin{Bmatrix} U_{mn} \cos(\mu x) \sin(\beta y) \\ V_{mn} \sin(\mu x) \cos(\beta y) \\ W_{mn} \sin(\mu x) \sin(\beta y) \\ X_{mn} \sin(\mu x) \sin(\beta y) \end{Bmatrix} \tag{29}$$

Where U_{mn}, V_{mn}, W_{mn}, X_{mn} are arbitrary parameters to be determined. μ and β are defined as

$$\mu = \frac{m\pi}{a} \ et \ \beta = \frac{n\pi}{b} \tag{30}$$

Substituting Eq. (29) into Eq. (19) as function of displacements terms, the closed-form solution of buckling load of the FG-sandwich plate can be obtained from

$$\begin{bmatrix} a_{11} & a_{12} & a_{13} & a_{14} \\ a_{12} & a_{22} & a_{23} & a_{24} \\ a_{13} & a_{23} & a_{33} & a_{34} \\ a_{14} & a_{24} & a_{34} & a_{44} \end{bmatrix} \begin{Bmatrix} U_{mn} \\ V_{mn} \\ W_{mn} \\ X_{mn} \end{Bmatrix} = \begin{Bmatrix} 0 \\ 0 \\ 0 \\ 0 \end{Bmatrix} \tag{31}$$

where

$$\begin{gathered} a_{11} = -(A_{11}\mu^2 + A_{66}\beta^2) \\ a_{12} = -\mu\, \beta\, (A_{12} + A_{66}) \\ a_{13} = \mu(B_{11}\mu^2 + (B_{12} + 2B_{66})\beta^2) \\ a_{14} = -\mu(B_{11}^s A' k_1 \mu^2 + B_{12}^s B' k_2 \beta^2 \\ + B_{66}^s (A' k_1 + B' k_2)\beta^2) \\ a_{22} = -\mu^2 A_{66} - \beta^2 A_{22} \\ a_{23} = \beta(B_{22}\beta^2 + (B_{12} + 2B_{66})\mu^2) \\ a_{24} = \\ -\beta\left(B_{22}^s B' k_2 \beta^2 + \mu^2\left(B_{12}^s A' k_1 + B_{66}^s (A' k_1 + B' k_2)\right)\right) \\ a_{33} = -\mu^2(D_{11}\mu^2 + (2D_{12} + 4D_{66})\beta^2) \\ -D_{22}\beta^4 + N_x^0\mu^2 + N_y^0\beta^2 - K_w - K_p(\mu^2 + \beta^2) \\ a_{34} = D_{11}^s A' k_1 \mu^4 + D_{12}^s (A' k_1 + B' k_2)\beta^2\mu^2 \\ + D_{22}^s B' k_2 \beta^4 + 2D_{66}^s (A' k_1 + B' k_2)\beta^2\mu^2 \\ a_{44} = -(H_{11}^s \mu^2 k_1 + 2k_1\beta^2 H_{66}^s + 2H_{66}^s \mu^2 k_2 \\ + H_{12}^s \mu^2 k_2 + k_1 \beta^2 H_{12}^s + k_2 \beta^2 H_{22}^s + A_s^{44} k_1 + A_s^{55} k_2) \end{gathered} \tag{32}$$

In order to obtain the non-trivial solution, the determinant $|A|$ should be zero. By solving the equation $|A| = 0$, we can easily obtain the buckling load $\bar{N} = P_x$ and the buckling temperature $\Delta T_{cr}(P_x = P_y = 0)$.

4. Numerical results

The numerical results of the mechanical and hygrothermal buckling analysis of SS-FG sandwich plate are presented in the following section. The FG-material continuously varies from the silicon nitride (Si_3N_4) to stainless steel (SUS304). The properties of each material are abstracted in the Table 1.

Table 1 properties of FG plate components

Materials	Silicon nitride (Si_3N_4)	Stainless steel (SUS304)
E [GPa]	348.43	201.04
α[x10^{-6}/°C]	5.8711	12.330
$K\ [W/mK]$	13.723	15.379
$\beta(wt\ \%H_2O)^{-1}$	0.001	0.44
ν	0.3	

The temperature in the bottom surface is taken $T_b = 25$°C.

All results presented in this work are computed in the non-dimensional form as

$$\begin{gathered} N_{cr} = \frac{\bar{N}b}{D_c}, \quad \bar{N}_{cr} = \frac{\bar{N}a^2}{bh^3E_m}, \quad T_{cr} = 10^{-3}\Delta T_{cr} \\ J_1 = \frac{K_w a^4}{D_c}, \quad J_2 = \frac{K_p a^2}{D_c}, \quad D_c = \frac{E_c h^3}{12(1-\nu^2)} \\ \bar{J}_1 = \frac{K_w a^4}{D_m}, \quad \bar{J}_2 = \frac{K_p a^2}{D_m}, \quad D_m = \frac{E_m h^3}{12(1-\nu^2)} \\ \xi = \frac{H_c}{H_f} \end{gathered} \tag{33}$$

The material properties used in Tables 3 and 4 are $E_c = 380$ GPa, $\alpha_c = 7.4\text{x}10^{-6}/°\text{C}$, $E_m = 70$ GPa, and $\alpha_m = 23x10^{-6}/°C$; while the material properties used in Table 5 are $E_c = 244.27$ GPa, $\alpha_c = 12.766\text{x}10^{-6}/°\text{C}$, $E_m = 66.2$ GPa, $\alpha_m = 10.3x10^{-6}/°C$.

4.1 Plate subjected to mechanical loads

For verification of the theory used, the obtained results for mechanical buckling of homogeneous and FG-plate are compared with those found in the literature.

The Table 2 shows the comparison of the obtained critical buckling load N_{cr} of simply supported homogeneous with those computed via first-shear deformation theory (FSDT) of Akhavan *et al.* (2009) and TSDT model of (Thai and Kim 2013, Yaghoobi and Fereidoon 2014) and RPT of Radwan (2017). From the Table 1, it can be seen for all aspect ratio '*a/b*', geometry ratio '*a/h*' and elastic-foundation parameter (J_1,J_2) that the current results are in good agreement with those given by (Akhavan *et al.* 2009, Thai and Kim 2013, Yaghoobi and Fereidoon 2014, Radwan 2017).

The nondimensional critical buckling load 'N_{cr}' of simply-supported square FG-plate under compressive load is presented in the Table 3. The results computed using the present hyperbolic-HSDT are compared with refined nth-order shear deformation theory developed by Yaghoobi and Fereidoon (2014), the TSDT proposed by Thai and Kim (2013) and RPT of Radwan (2017). It is clear from the table that the current model gives almost the same values as the other models in the literature. It is also remarkable that the non-dimensional critical buckling load 'N_{cr}' is in inverse

Table 2 Comparison of non-dimensional buckling load N_{cr} of a homogeneous rectangular plate on elastic foundations (R=0, n=1)

a/b	J_1	J_2	Theory	*a/h*			
				5	10	100	1000
0.5	0	0	Akhavan *et al*. (2009)	54.3207	59.6629	61.6641	61.6848
			Thai and Kim (2013)	54.0737	59.5856	61.6633	61.6848
			Yaghoobi and Fereidoon (2014)	54.0737	59.5860	61.6633	61.6848
			Radwan (2017)	54.0780	59.5873	61.6633	61.6848
			Present	54,0859	59,5887	61,6633	61,6848
	100	10	Akhavan *et al*. (2009)	144.6952	150.1910	152.1930	152.2130
			Thai and Kim (2013)	144.6022	150.1141	152.1918	152.2133
			Yaghoobi and Fereidoon (2014)	144.6022	150.1141	152.1918	152.2133
			Radwan (2017)	144.6065	150.1158	152.1918	152.2133
			Present	144,6144	150,1172	152,1918	152,2132
	1000	100	Akhavan *et al*. (2009)	*643.5000*^{b}	686.1710^a	704.3860^a	704.5890^a
			Thai and Kim (2013)	640.9782^b	685.5369^a	704.3775^a	704.5888^a
			Yaghoobi and Fereidoon (2014)	640.9782^b	685.5369^a	704.3775^a	704.5888^a
			Radwan (2017)	640.8714^b	685.5487^a	704.3777^a	704.5888^a
			Present	641,3795^b	685,5670^a	704,3778^a	704,5887^a
1	0	0	Akhavan *et al*. (2009)	32.4414	37.4477	39.4570	39.4782
			Thai and Kim (2013)	32.2276	37.3721	39.4562	39.4782
			Yaghoobi and Fereidoon (2014)	32.2276	37.3721	39.4562	39.4782
			Radwan (2017)	32.2305	37.3738	39.4562	39.4782
			Present	32,2398	37,3753	39,4562	39,4781
	100	10	Akhavan *et al*. (2009)	55.0289^a	67.5798	69.5891	69.6103
			Thai and Kim (2013)	54.5692^a	67.5042	69.5883	69.6103
			Yaghoobi and Fereidoon (2014)	54.5692^a	67.5042	69.5883	69.6103
			Radwan (2017)	54.5665^a	67.5059	69.5883	69.6103
			Present	54,6116^a	67,5074	69,5883	69,6103
	1000	100	Akhavan *et al*. (2009)	174.9760^b	204.6510^a	211.9610^a	212.0140^a
			Thai and Kim (2013)	174.2676^b	204.4040^a	211.9285^a	212.0145^a
			Yaghoobi and Fereidoon (2014)	174.2676^b	204.4040^a	211.9285^a	212.0145^a
			Radwan (2017)	174.2320^b	204.4084^a	211.9285^a	212.0145^a
			Present	174,3907^b	204,4162^a	211,9286^a	212,0144^a
2	0	0	Akhavan *et al*. (2009)	19.2255^b	32.4414^a	39.3930^a	39.4776^a
			Thai and Kim (2013)	18.9794^b	32.2276^a	39.3896^a	39.4775^a
			Yaghoobi and Fereidoon (2014)	18.9794^b	32.2276^a	39.3896^a	39.4775^a
			Radwan (2017)	18.9574^b	32.2305^a	39.3896^a	39.4775^a
			Present	19,0400	32,2398^a	39,3896^a	39,4775^a
	100	10	Akhavan *et al*. (2009)	22.7476^c	37.5182^b	45.0262^a	45.1108^a
			Thai and Kim (2013)	22.5785^c	37.8358^b	45.0228^a	45.1108^a
			Yaghoobi and Fereidoon (2014)	22.5785^c	37.8358^b	45.0228^a	45.1108^a
			Radwan (2017)	22.5322^c	*37.8377*^{b}	45.0229^a	45.1108^a
			Present	22,6777^c	37,8580^b	45,0229^a	45,1107^a
	1000	100	Akhavan *et al*. (2009)	--	72.8290^c	85.0953^b	85.2563^b
			Thai and Kim (2013)	50.0214^d	72.3694^c	85.0887^b	85.2562^b
			Yaghoobi and Fereidoon (2014)	50.0214^d	72.3694^c	85.0887^b	85.2562^b
			Radwan (2017)	49.9393^d	72.3667^c	85.0888^b	85.2562^b
			Present	50,1748^d	72,4117^c	85,0889^b	85,2562^b

The superscripts *a*, *b*, *c* and *d* denote m=2, 3, 4 and 5

relation with the material index. It can be noted that the presence of the elastic-foundation makes the plate more rigid.

The critical buckling load 'N_{cr}' of the FG-sandwich plate reposed on elastic-foundation versus the geometry ratio '*a/h*', aspect ratio '*b/a*' and load ratio '*R*' is plotted in the Fig. 2. The FG-sandwich plate has (k=1, ξ=1, J_1=100, J_2=10). It can be seen from the plotted curves that the

Table 3 Comparison of non-dimensional critical buckling load Ncr of square FG-plate on elastic foundations (R=1, a/h=10)

J_1	J_2	Theory	K					
			0	0.5	1	2	5	10
0	0	Thai and Kim (2013)	9.2893	6.0615	4.6695	3.6315	3.0177	2.7264
		Yaghoobi and Fereidoon (2014)	9.2893	6.0615	4.6695	3.6315	3.0177	2.7264
		Radwan (2017)	9.2897	6.0617	4.6697	3.6321	3.0195	2.7275
		Present	9,2902	6,0619	4,6699	3,6325	3,0206	2,7282
100	10	Thai and Kim (2013)	10.6689	7.4411	6.0492	5.0112	4.3973	4.1061
		Yaghoobi and Fereidoon (2014)	10.6689	7.4411	6.0492	5.0112	4.3973	4.1061
		Radwan (2017)	10.6693	7.4413	6.0494	5.0118	4.3992	4.1071
		Present	10,6699	7,4416	6,0496	5,0122	4,4002	4,1078
1000	100	Thai and Kim (2013)	23.0860	19.8582	18.4663	17.4283	16.8144	16.5232
		Yaghoobi and Fereidoon (2014)	23.0860	19.8582	18.4663	17.4283	16.8144	16.5232
		Radwan (2017)	23.0864	19.8584	18.4665	17.4289	16.8162	16.5242
		Present	23,0870	19,8587	18,4667	17,4293	16,8174	16,5250

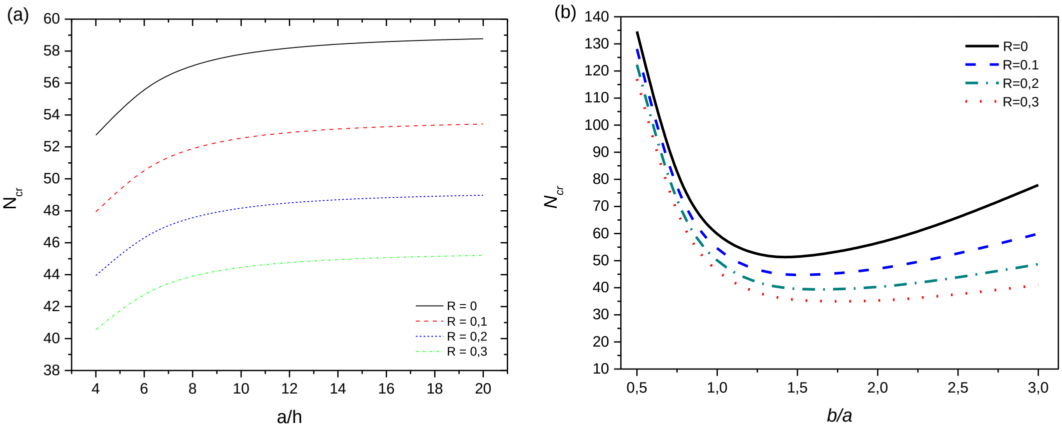

Fig. 2 Buckling load parameter 'N_{cr}' of FG-sandwich plate vs. (a) the side-to-thickness ratio a/h (b/a=1) and (b) aspect ratio b/a (a/h=10) for various load ratios (k=1, ξ=1, J_1=100, J_2=10)

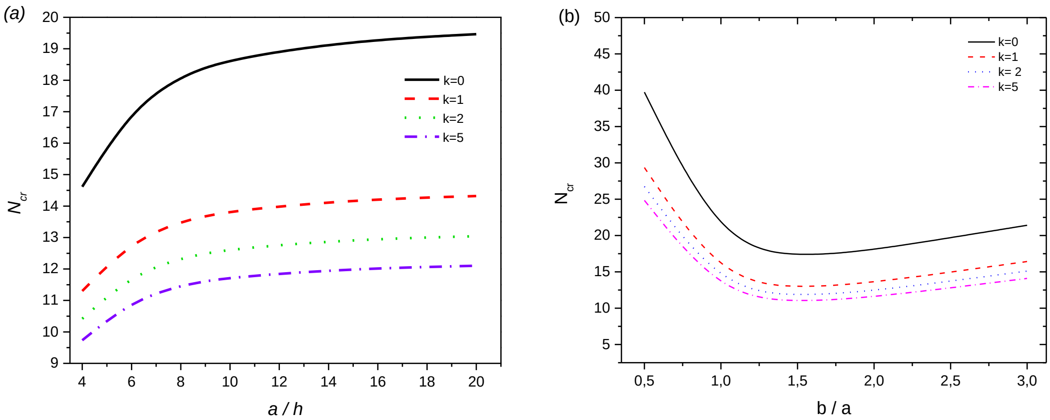

Fig. 3 Buckling load parameter 'N_{cr}' of FG-sandwich plates under biaxial compression (R=1) vs. (a) the side-to-thickness ratio a/h (b/a=1) and (b) aspect ratio b/a (a/h=10) for various values of the power law index k with (ξ=1, J_1=J_2=0)

critical buckling load 'N_{cr}' is in direct correlation relation with geometry ratio 'a/h' and decrease with increasing of the aspect ratio 'b/a' to a minimum value corresponding to 'b/a=1.5' then it increases. The biggest values of 'N_{cr}' is obtained for load ratio 'R=0'.

Fig. 3 shows the variation of the buckling load parameter 'N_{cr}' of the FG-sandwich plate without elastic-foundation (J_1=J_2=0) as function of the power index 'k', dimension 'b/a' and geometry 'a/h' ratios. From the graphs, it can be observed that the increasing in the power index 'k' and geometry ratio 'a/h' lead to an increase in the values of buckling load parameter 'N_{cr}', but this values decrease when the aspect ratio 'b/a' increase.

The Effect of the layer thickness ratio 'ξ' and dimension

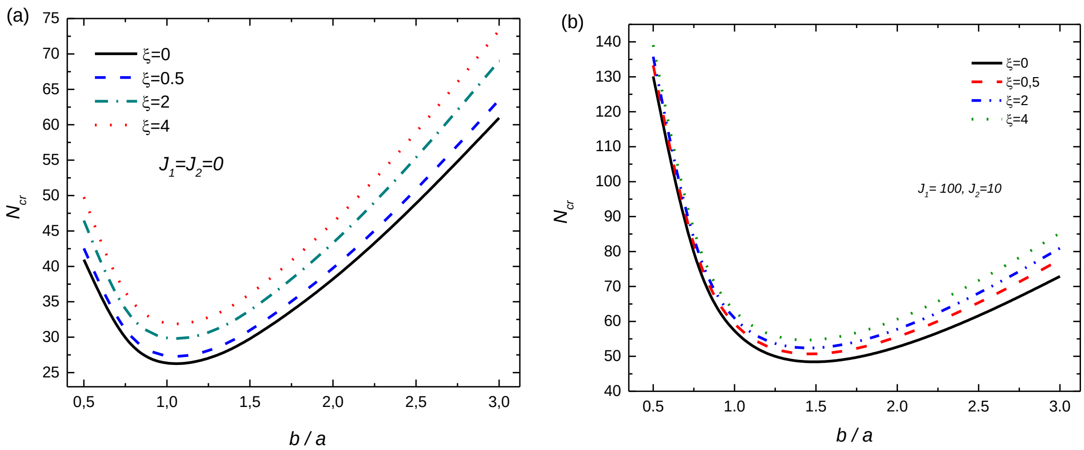

Fig. 4 Buckling load parameter 'N_{cr}' of FG-sandwich plates under uniaxial compression (R=0) vs. the aspect ratio b/a for various values of the core-to-face thickness ratio (a) without elastic foundations J_1=J_2=0 and (b) on elastic-foundations J_1=100, J_2=10 (k=1, a/h=10)

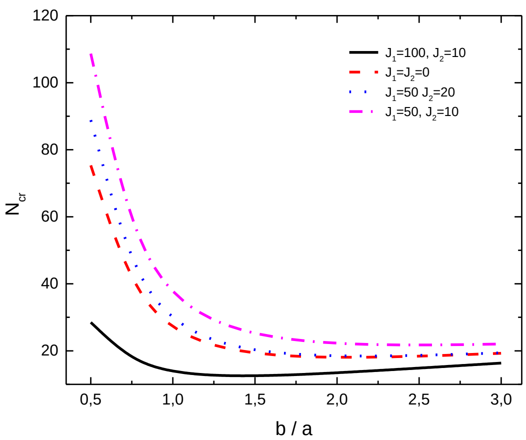

Fig. 5 Buckling load parameter 'N_{cr}' of FG-sandwich plates under biaxial compression (R=1) vs. the aspect ratio 'b/a' for various values of the elastic foundation parameters with (ξ=1, k=1, a/h=10)

ratio 'b/a' on the critical buckling load parameter 'N_{cr}' of the simply-supported FG-sandwich plates under uniaxial compressive load 'R=0' is presented in the Fig. 4. From the plotted curve, it can be observed that the values of the critical buckling load 'N_{cr}' of the FG-sandwich plate without elastic-foundations are smaller than FG-plate with elastic-foundation (J_1=100, J_2=10). It is clear also that the lower values of the buckling load parameter 'N_{cr}' is given by plate without core.

Fig. 5 reveal the variation of the critical buckling load 'N_{cr}' of the FG-sandwich plate under biaxial mechanical loads as function of the elastic-foundation parameter (J_1,J_2) and aspect ratio 'b/a'. It is remarkable from the graphs that the increase of the aspect ratio 'b/a' leads to decrease the values of the critical buckling load 'N_{cr}'. The FG-sandwich plate with elastic-foundation (J_1=50, J_2=10) give the greater values of the 'N_{cr}'.

Table 4 Comparison of non-dimensional critical buckling temperature 'T_{cr}' of square FG-plate on elastic foundations under uniform temperature rise

k	Theory	J_1=0, J_2=0			J_1=10, J_2=0			J_1=10, J_2=10		
		a/h=5	10	20	a/h=5	10	20	a/h=5	10	20
0	Yaghoobi and Torabi (2013)	5.58069	1.61862	0.42153	5.75623	1.66251	0.43251	9.22123	2.52876	0.64907
	Zenkour and Sobhy (2011)	5.58556	1.61882	0.42154	5.76109	1.66270	0.43252	9.22610	2.52896	0.64908
	Radwan (2017)	5.58394	1.61875	0.42154	5.75948	1.66264	0.43251	9.22448	2.52889	0.64907
	Present	5,56502	1,59416	0,39657	5,74056	1,63804	0,40754	9,20556	2,50429	0,62410
1	Zenkour and Sobhy (2011)	2.67241	0.75845	0.19627	2.83603	0.79935	0.20649	6.06558	1.60674	0.40834
	Radwan (2017)	2.67174	0.75842	0.19627	2.83535	0.79933	0.20649	6.06491	1.60672	0.40834
	Present	2,64926	0,73358	0,17128	2,81287	0,77449	0,18150	6,04243	1,58188	0,38335
5	Yaghoobi and Torabi (2013)	2.35948	0.68678	0.17905	2.58625	0.74347	0.19322	7.06257	1.86255	0.47299
	Zenkour and Sobhy (2011)	2.27131	0.67895	0.17851	2.49808	0.73564	0.19268	6.97440	1.85472	0.47245
	Radwan (2017)	2.27935	0.67972	0.17856	2.50612	0.73641	0.19274	6.98244	1.85549	0.47251
	Present	2,24462	0,65377	0,15350	2,47139	0,71046	0,16767	6,94771	1,82954	0,44744
10	Yaghoobi and Torabi (2013)	2.36822	0.70108	0.18373	2.62416	0.76507	0.19972	7.67626	2.02809	0.51548
	Zenkour and Sobhy (2011)	2.27551	0.69254	0.18313	2.53146	0.75653	0.19913	7.58356	2.01955	0.51489
	Radwan (2017)	2.27936	0.69296	0.18316	2.53531	0.75694	0.19916	7.58740	2.01997	0.51492
	Present	2,25119	0,66757	0,15814	2,50713	0,73156	0,17413	7,55922	1,99458	0,48989

Table 5 Comparison of non-dimensional critical buckling temperature 'T_{cr}' of the square FG-sandwich plates under non-linear temperature rise (γ=5)

ξ	k	Theory	a/h				
			5	10	15	25	50
0	0.5	Zenkour and Sobhy (2010)	21.61337	5.90995	2.58239	0.81982	0.06380
		Radwan (2017)	21.60648	5.90948	2.58230	0.81981	0.06380
		Present	21,60480	5,9093	2,58228	0,81981	0,06380
	2	Zenkour and Sobhy (2010)	3.02926	6.12449	2.64800	0.82107	0.04052
		Radwan (2017)	23.00135	6.12245	2.64759	0.82102	0.04051
		Present	22,98800	6,12147	2,64739	0,82100	0,04050
0.5	0.5	Zenkour and Sobhy (2010)	21.33821	5.83566	2.54875	0.80744	0.06048
		Radwan (2017)	21.33354	5.83536	2.54869	0.80743	0.06048
		Present	21,33300	5,83535	2,54869	0,80743	0,06048
	2	Zenkour and Sobhy (2010)	22.35275	5.89838	2.53488	0.77011	0.01668
		Radwan (2017)	22.33166	5.89686	2.53458	0.77007	0.01668
		Present	22,32160	5,89614	2,53443	0,77005	0,01668
1	0.5	Zenkour and Sobhy (2010)	21.12437	5.79091	2.53084	0.80247	0.06078
		Radwan (2017)	21.12333	5.79089	2.53084	0.80246	0.06078
		Present	21,12500	5,79100	2,53090	0,80247	0,06079
	2	Zenkour and Sobhy (2010)	21.98303	5.81247	2.49756	0.75699	0.01363
		Radwan (2017)	21.97101	5.81161	2.49738	0.75698	0.01363
		Present	21,96600	5,81120	2,49730	0,75697	0,01363
2	0.5	Zenkour and Sobhy (2010)	20.80375	5.73532	2.51144	0.79933	0.06402
		Radwan (2017)	20.80829	5.73575	2.51152	0.79935	0.06403
		Present	20,81300	5,73610	2,51160	0,79936	0,06403
	2	Zenkour and Sobhy (2010)	21.54679	5.75368	2.48202	0.75946	0.02279
		Radwan (2017)	21.54827	5.75383	2.48206	0.75946	0.02279
		Present	21,55000	5,75400	2,48210	0,75947	0,02279

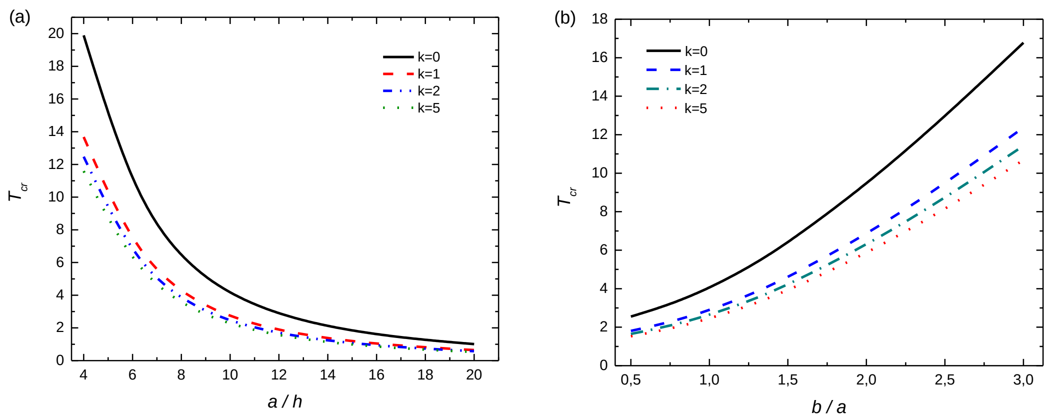

Fig. 6 Buckling temperature change 'T_{cr}' of FG-sandwich plates under linear temperature distribution (γ=1) vs. (a) the side-to-thickness ratio a/h (b/a=1) and (b) aspect ratio b/a (a/h=10) for various values of the power law index 'k' with (ξ=1, J_1=J_2=0)

4.2 Plate subjected to hygrothermal loads

In this section, the obtained results of the critical buckling temperature 'T_{cr}' of functionally graded and FG-sandwich plates are compared with those available in the literature.

The Table 4 presents the critical buckling temperature 'T_{cr}' of the FG-plate without and with elastic-foundation under uniform-thermal load. The computed results are compared with those given by Yaghoobi and Torabi (2013), Zenkour and Sobhy (2011) and Radwan 2017 using the FSDT, TSDT and RPT, respectively. It can be noted from the table that the increase in the values of material index 'k' leads to reduce the critical buckling temperature 'T_{cr}' and this is confirmed for FG-plate with and without elastic-foundation.

Table 5 demonstrates the comparison of the critical buckling temperature 'T_{cr}' of the FG-sandwich plate under non-linear thermal load with (γ=5). It can be observed from this table that the non-dimensional critical buckling temperature 'T_{cr}' is in direct correlation relation with power index 'k'. it can be confirmed again that the present results

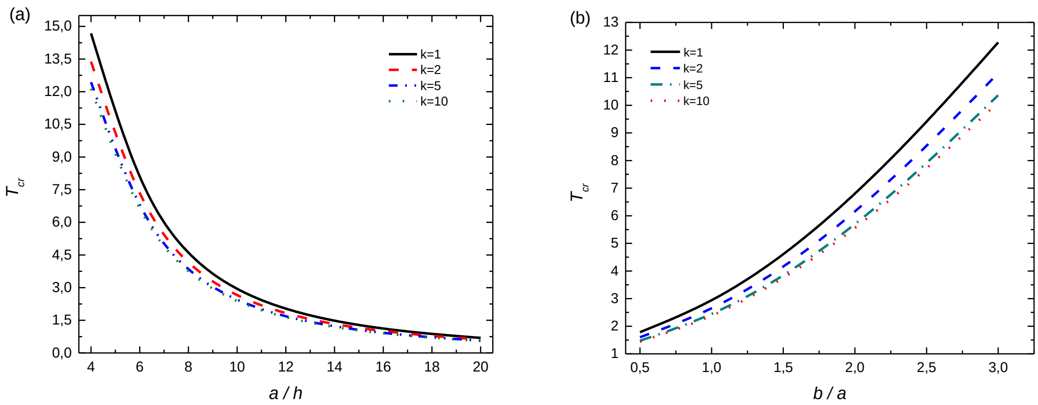

Fig. 7 Buckling temperature change 'T_{cr}' of FG-sandwich plates under non-linear Fourier temperature distribution vs. (a) the side-to-thickness ratio a/h (b/a=1) and (b) aspect ratio b/a (a/h=10) for various values of the power law index 'k' with (ξ=1, J_1=J_2=0)

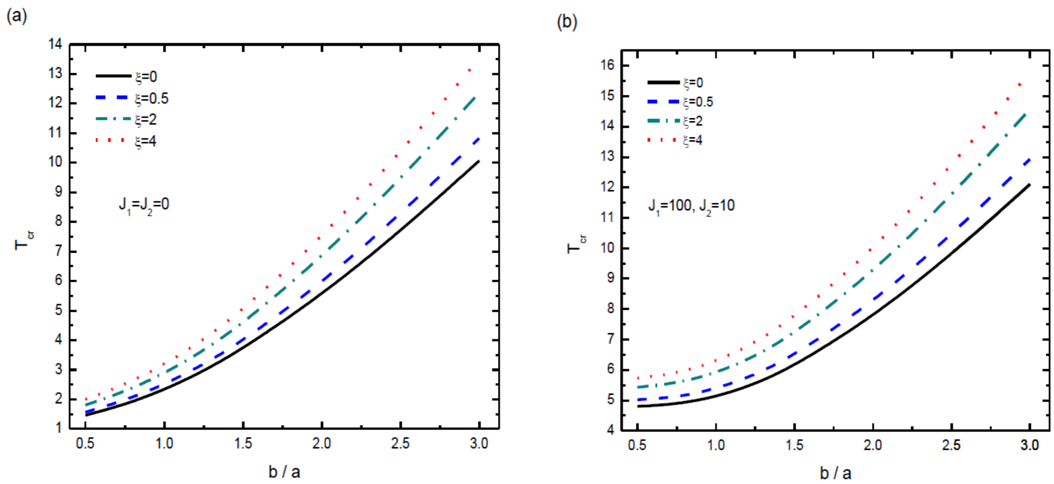

Fig. 8 Buckling temperature change 'T_{cr}' of FG-sandwich plates under linear temperature distribution (γ=1) vs. the aspect ratio b/a for various values of the core-to-face thickness ratio ξ (a) without elastic foundations J_1=J_2=0 and (b) on elastic foundations J_1=100, J_2=10 with (k=1, a/h=10)

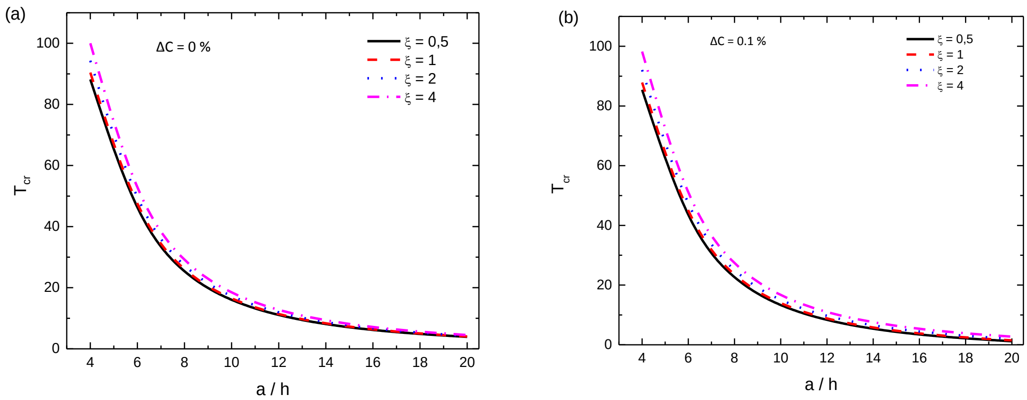

Fig. 9 Buckling temperature change 'T_{cr}' of FG-sandwich plates under non-linear Fourier temperature distribution vs. the side-to-thickness ratio a/h (a) thermal buckling and (b) hygrothermal buckling for various values of the core-to-face thickness ratio ξ with (k=1, b/a=1, J_1=100, J_2=10)

are almost the same with those given by Zenkour and Sobhy (2010) and Radwan (2017). The lower values of the critical buckling temperature 'T_{cr}' are obtained when the core thickness of the FG-sandwich plate is twice as large as the faces sheet.

The critical buckling temperatures 'T_{cr}' of the simply-supported square FG-sandwich plate under linear and non-linear thermal load versus the power index 'k', aspect 'a/b' and geometry ratios 'a/h' are presented in the Figs. 6 and 7, respectively. From the obtained results, it can be

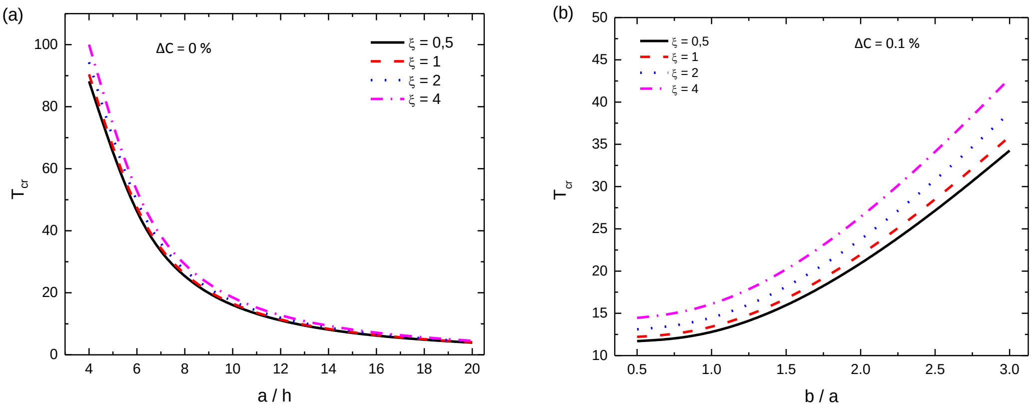

Fig. 10 Buckling temperature change 'T_{cr}' of FG-sandwich plates under non-linear Fourier temperature distribution vs. plate aspect ratio *b/a*: (a) thermal buckling and (b) hygrothermal buckling for various values of the core-to-face thickness ratio ξ with (k=1, a/h=10, J_1=100, J_2=10)

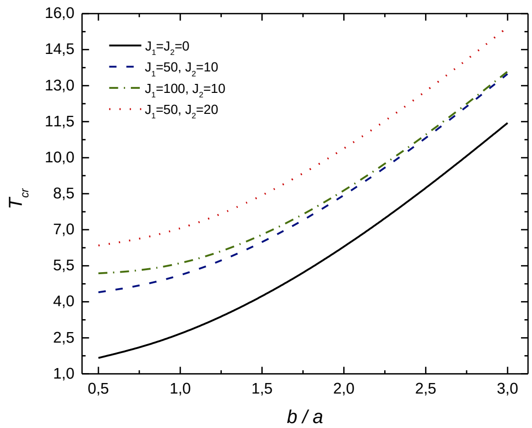

Fig. 11 Buckling temperature change 'T_{cr}' of FG-sandwich plate under linear temperature distribution (γ=1) vs. the aspect ratio '*b/a*' for various values of the elastic foundation parameters with (ξ=1, k=1, a/h=10)

concluded that the values critical buckling temperatures 'T_{cr}' decrease with increasing of the power index 'k' and geometry ratio '*a/h*' and the aspect ratio lead to an increase in the values of the buckling temperature 'T_{cr}'.

Figs. 8-10 shows the effect of the aspect '*b/a*', geometry '*a/h*' and layer thickness 'ξ' ratios on the thermal buckling load of the FG-sandwich plate under hygrothermal, linear (γ=1) and non-linear thermal distributions. The FG-sandwich plate is seated on the elastic-foundation with (J_1=100, J_2=10) and the power index is taken 'k=1'. The current results shows that the critical buckling temperature 'T_{cr}' increase with increasing of the ratio '*b/a*' and decrease with increasing of the ratio '*a/h*'. it can be also noted that the larger values of the 'T_{cr}' are obtained for the FG-sandwich plate with ξ=4. We can also conclude that the presence of the moisture leads to a reduction in the values of 'T_{cr}'.

Fig. 11 present the variation of the thermal buckling load 'T_{cr}' of the FG-sandwich plate under linear temperature distribution (γ=1) versus the aspect ratio '*b/a*' and elastic-foundation parameter (J_1,J_2). It can be observed from the plotted graphs that the thermal buckling load 'T_{cr}' increase with increasing of the aspect ratio '*b/a*'. The FG-sandwich plate without elastic-foundation (J_1=0, J_2=0) the give the smaller values of the thermal buckling load 'T_{cr}'.

Figs. 12 and 13 presents the critical buckling hygrothermal load 'T_{cr}' of FG-sandwich plate with (ξ=1, k=1, J_1=100, J_2=10) under thermal and moisture loads versus non-linearity index 'γ' , aspect and geometry ratios. It can be seen from the obtained results that the critical buckling hygrothermal load 'T_{cr}' is in direct correlation relation with index 'γ' and this is confirmed for various values of the moisture. It can be also concluded that critical buckling hygrothermal load 'T_{cr}' decrease with increasing of the parameter '*a/h*' and increase with increasing of the parameter '*b/a*'.

The effect of the moisture concentration 'ΔC', aspect and geometry ratios on the buckling temperature 'T_{cr}' of thick FG-sandwich plates (γ=1, k=1, ξ=1) resting on elastic-foundations is presented in the Fig. 14. From the plotted curves, it can be noted the buckling temperature 'T_{cr}' is in inverse relation with the moisture concentration 'ΔC' and geometry ratio '*a/h*'. It can be confirmed again that the increasing in the values of the parameter '*b/a*' leads to an increase of the values of the 'T_{cr}'.

5. Conclusions

In the present paper, the mechanical and hygrothermal stability of the simply-supported FG-sandwich plate seated on elastic-foundations is investigated using a novel hyperbolic shear deformation theory. The equations of stability of the FG-sandwich plate are derived and solved via virtual-work principle and Navier method, respectively. From the computed results and comparisons, it can be conclude that the current 2D-integral hyperbolic shear deformation theory is accurate and effective to predictthe critical buckling load of the FG-sandwich plate subjected to mechanical and hygrothermal loads. Finally several parametric studies are presented to show the various factors influencing on the stability of the simply-supported FG-sandwich plate. Finally, an improvement of the current approach will be employed in the future work to consider other type of materials (Sedighi *et al.* 2012a, b, 2013,

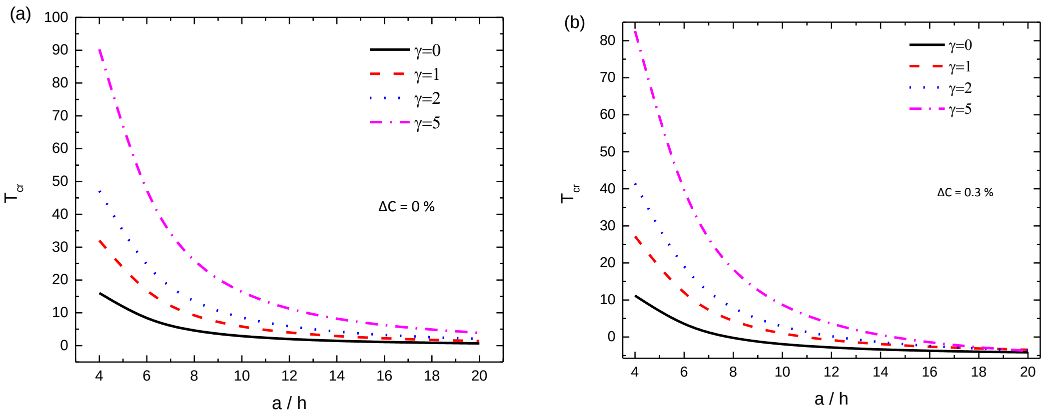

Fig. 12 Buckling hygrothermal change ‘T_{cr}’ of FG-sandwich plates under various temperature and moisture loads: (a) thermal load and (b) hygrothermal loads with (b/a=1, ξ=1, k=1, J_1=100, J_2=10)

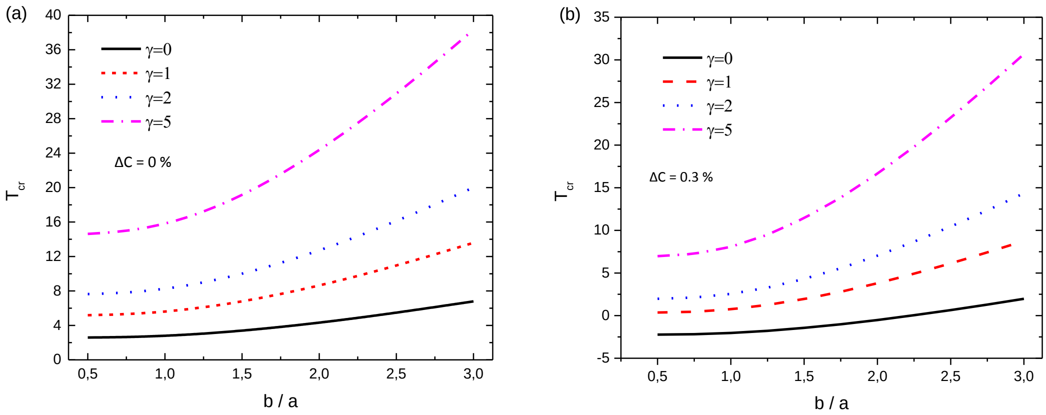

Fig. 13 Buckling hygrothermal change ‘T_{cr}’ of FG-sandwich plates under various temperature and moisture loads: (a) thermal load and (b) hygrothermal loads with (a/h=10, ξ=1, k=1, J_1=100, J_2=10)

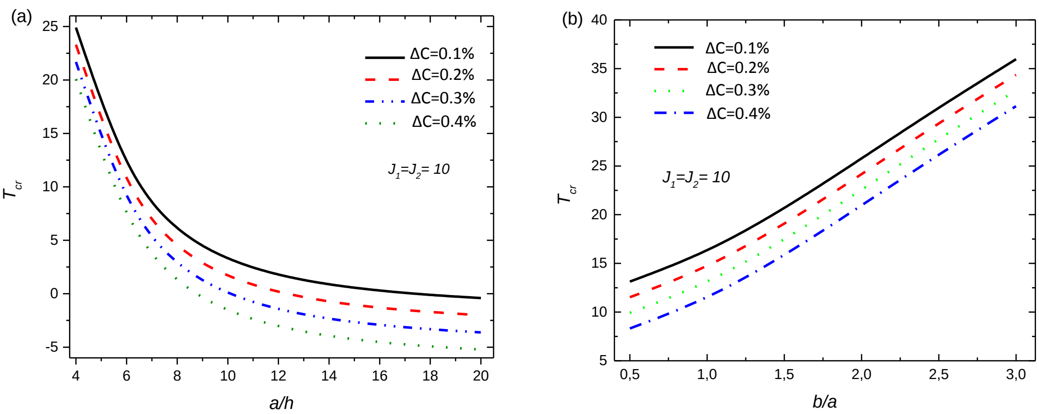

Fig. 14 Effect of the moisture concentration ‘ΔC’ on the buckling temperature ‘T_{cr}’ of FG-sandwich plate resting on elastic-foundations vs. (a) the side-to-thickness ‘a/h’ (b/a=1) and (b) aspect ratio ‘b/a’ (a/h=10) with (γ=1, k=1, ξ=1, a/h=5)

Abdelmalek *et al*. 2017, Daouadji 2017, Narwariya *et al*. 2018, Behera and Kumari 2018, Belkacem *et al*. 2018, Belmahi *et al*. 2018, Dihaj *et al*. 2018, Hamidi *et al*. 2018, Othman and Mahdy 2018, Bensattalah *et al*. 2018a, b, Ayat *et al*. 2018, Faleh *et al*. 2018, Panjehpour *et al*. 2018, Al-Osta 2019, Yazdani and Mohammadimehr 2019, Hamad *et al*. 2019, Al-Maliki *et al*. 2019, Fenjan *et al*. 2019, Bensattalah *et al*. 2019a, b, Belmahi *et al*. 2019, Barati *et al*. 2019, Akbas 2019c, Othman *et al*. 2019, Abdou *et al*. 2019, Eltaher *et al*. 2019, 2020, Forsat *et al*. 2020, Faleh *et al*. 2020).

References

Abdelmalek, A., Bouazza, M., Zidour, M. and Benseddiq, N. (2019), “Hygrothermal effects on the free vibration behavior of composite plate using *n*th-order shear deformation theory: a micromechanical approach", *Iran. J. Sci. Technol. Tran. Mech. Eng.*, **43**, 61-73. https://doi.org/10.1007/s40997-017-0140-y.

Abdou, M.A., Othman, M.I.A., Tantawi, R.S. and Mansour, N.T. (2019), "Exact solutions of generalized thermoelastic medium with double porosity under L-S theory", *Indi. J. Phys.*, 1-12. https://doi.org/10.1007/s12648-019-01505-8.

Akavci, S.S. (2016), "Mechanical behavior of functionally graded sandwich plates on elastic foundation", *Compos. Part B: Eng.*, **96**, 136-152. https://doi.org/10.1016/j.compositesb.2016.04.035.

Akbaş, S.D. (2017), "Vibration and static analysis of functionally graded porous plates", *J. Appl. Comput. Mech.*, **3**(3), 199-207. https://doi.org/10.22055/JACM.2017.21540.1107.

Akbas, S.D. (2019a), "Forced vibration analysis of functionally graded sandwich deep beams", *Coupl. Syst. Mech.*, **8**(3), 259-271. https://doi.org/10.12989/csm.2019.8.3.259.

Akbas, S.D. (2019b), "Hygro-thermal post-buckling analysis of a functionally graded beam", *Coupl. Syst. Mech.*, **8**(5), 459-471. https://doi.org/10.12989/csm.2019.8.5.459.

Akbaş, S.D. (2019c), "Nonlinear static analysis of laminated composite beams under hygro-thermal effect", *Struct. Eng. Mech.*, **72**(4), 433-441. https://doi.org/10.12989/sem.2019.72.4.433.

Akhavan, H., Hashemi, S.H., Taher, H.R.D., Alibeigloo, A. and Vahabi, S. (2009), "Exact solutions for rectangular Mindlin plates under in-plane loads resting on Pasternak elastic foundation. Part II: Frequency analysis", *Comput. Mater. Sci.*, **44**(3), 951-961. https://doi.org/10.1016/j.commatsci.2008.07.001.

Al-Maliki, A.F., Faleh, N.M. and Alasadi, A.A. (2019) "Finite element formulation and vibration of nonlocal refined metal foam beams with symmetric and non-symmetric porosities", *Struct. Monit. Maintain.*, **6**(2), 147-159. https://doi.org/10.12989/smm.2019.6.2.147.

Al-Osta, M.A. (2019), "Shear behaviour of RC beams retrofitted using UHPFRC panels epoxied to the sides", *Comput. Concrete*, **24**(1), 37-49. https://doi.org/10.12989/cac.2019.24.1.037.

Ayat, H., Kellouche, Y., Ghrici, M. and Boukhatem, B. (2018), "Compressive strength prediction of limestone filler concrete using artificial neural networks", *Adv. Comput. Des.*, **3**(3), 289-302. https://doi.org/10.12989/acd.2018.3.3.289.

Barati, M.R. and Shahverdi, H. (2019), "Finite element forced vibration analysis of refined shear deformable nanocompositegraphene platelet-reinforced beams", *J. Brazil. Soc. Mech. Sci. Eng.*, **42**(1), 33. https://doi.org/10.1007/s40430-019-2118-8.

Behera, S. and Kumari, P. (2018), "Free vibration of Levy-type rectangular laminated plates using efficient zig-zag theory", *Adv. Comput. Des.*, **3**(3), 213-232. https://doi.org/10.12989/acd.2017.2.3.165.

Belkacem, A., Tahar, H.D., Abderrezak, R., Amine, B.M., Mohamed, Z. and Boussad, A. (2018), "Mechanical buckling analysis of hybrid laminated composite plates under different boundary conditions", *Struct. Eng. Mech.*, **66**(6), 761-769. https://doi.org/10.12989/sem.2018.66.6.761.

Belmahi, S., Zidour, M. and Meradjah, M. (2019), "Small-scale effect on the forced vibration of a nano beam embedded an elastic medium using nonlocal elasticity theory", *Adv. Aircraf. Spacecraft Sci.*, **6**(1), 1-18. https://doi.org/10.12989/aas.2019.6.1.001.

Belmahi, S., Zidour, M., Meradjah, M., Bensattalah, T. and Dihaj, A. (2018), "Analysis of boundary conditions effects on vibration of nanobeam in a polymeric matrix", *Struct. Eng. Mech.*, **67**(5), 517-525. https://doi.org/10.12989/sem.2018.67.5.517.

Beni, N.N. (2019), "Free vibration analysis of annular sector sandwich plates with FG-CNT reinforced composite face-sheets based on the Carrera's Unified Formulation", *Compos. Struct.*, **214**, 269-292. https://doi.org/10.1016/j.compstruct.2019.01.094.

Bensattalah, T., Bouakkaz, K., Zidour, M. and Daouadji, T.H. (2018a), "Critical buckling loads of carbon nanotube embedded in Kerr's medium", *Adv. Nano Res.*, **6**(4), 339-356. https://doi.org/10.12989/anr.2018.6.4.339.

Bensattalah, T., Zidour, M. and Daouadji, T.H. (2019a), "A new nonlocal beam model for free vibration analysis of chiral single-walled carbon nanotubes", *Compos. Mater. Eng.*, **1**(1), 21-31. https://doi.org/10.12989/cme.2019.1.1.021.

Bensattalah, T., Zidour, M. and Hassaine Daouadji, T. (2018b), "Analytical analysis for the forced vibration of CNT surrounding elastic medium including thermal effect using nonlocal Euler-Bernoulli theory", *Adv. Mater. Res.*, **7**(3), 163-174. https://doi.org/10.12989/amr.2018.7.3.163.

Bensattalah, T., Zidour, M., Hassaine Daouadji, T. and Bouakaz, K. (2019b), "Theoretical analysis of chirality and scale effects on critical buckling load of zigzag triple walled carbon nanotubes under axial compression embedded in polymeric matrix", *Struct. Eng. Mech.*, **70**(3), 269-277. https://doi.org/10.12989/sem.2019.70.3.269.

Borsellino, C., Calabrese, L. and Valenza, A. (2004), "Experimental and numerical evaluation of sandwich composite structures", *Compos. Sci. Technol.*, **64**(10-11), 1709-1715. https://doi.org/10.1016/j.compscitech.2004.01.003.

Burlayenko, V.N. and Sadowski, T. (2019), "Free vibrations and static analysis of functionally graded sandwich plates with three-dimensional finite elements", *Meccanica*, **52**, 30-43. https://doi.org/10.1007/s11012-019-01001-7.

Chakrabarti, A. and Sheikh, A.H. (2005), "Analysis of laminated sandwich plates based on interlaminar shear stress continuous plate theory", *J. Eng. Mech.*, **131**(4), 377-384. https://doi.org/10.1061/(asce)0733-9399(2005)131:4(377).

Daouadji, T.H. (2017), "Analytical and numerical modeling of interfacial stresses in beams bonded with a thin plate", *Adv. Comput. Des.*, **2**(1), 57-69. https://doi.org/10.12989/acd.2017.2.1.057.

Dihaj, A., Zidour, M., Meradjah, M., Rakrak, K., Heireche, H. and Chemi, A. (2018), "Free vibration analysis of chiral double-walled carbon nanotube embedded in an elastic medium using non-local elasticity theory and Euler Bernoulli beam model", *Struct. Eng. Mech.*, **65**(3), 335-342. https://doi.org/10.12989/sem.2018.65.3.335.

Ebrahimi, F. and Barati, M.R. (2017a), "Buckling analysis of nonlocal strain gradient axially functionally graded nanobeams resting on variable elastic medium", *Proc. Inst. Mech. Eng., Part C: J. Mech. Eng. Sci.*, **232**(11), 2067-2078. https://doi.org/10.1177/0954406217713518.

Ebrahimi, F. and Barati, M.R. (2017b), "Scale-dependent effects on wave propagation in magnetically affected single/double-layered compositionally graded nanosize beams", *Wav. Rand. Complex Media*, **28**(2), 326-342. https://doi.org/10.1080/17455030.2017.1346331.

Eltaher, M.A. and Mohamed, S.A. (2020), "Buckling and stability analysis of sandwich beams subjected to varying axial loads", *Steel Compos. Struct.*, **34**(2), 241-260. https://doi.org/10.12989/scs.2020.34.2.241.

Eltaher, M.A., Almalki, T.A., Almitani, K.H., Ahmed, K.I.E. and Abdraboh, A.M. (2019), "Modal participation of fixed-fixed single-walled carbon nanotube with vacancies", *Int. J. Adv. Struct. Eng.*, **11**, 151-163. https://doi.org/10.1007/s40091-019-0222-8.

Eltaher, M.A., Mohamed, S.A. and Melaibari, A. (2020), "Static stability of a unified composite beams under varying axial loads", *Thin Wall. Struct.*, **147**, 106488. https://doi.org/10.1016/j.tws.2019.106488.

Emdadi, M., Mohammadimehr, M. and Navi, B.N. (2019), "Free vibration of an annular sandwich plate with CNTRC face sheets and FG porous cores using Ritz method", *Adv. Nano Res.*, **7**(2), 109-123. https://doi.org/10.12989/anr.2019.7.2.109.

Faleh, N.M., Ahmed, R.A. and Fenjan, R.M. (2018), "On vibrations of porous FG nanoshells", *Int. J. Eng. Sci.*, **133**, 1-14.

Faleh, N.M., Fenjan, R.M. and Ahmed, R.A. (2020), "Forced vibrations of multi-phase crystalline porous shells based on strain gradient elasticity and pulse load effects", *J. Vib. Eng. Technol.*, 1-9. https://doi.org/10.1007/s42417-020-00203-8.

Fenjan, R.M., Ahmed, R.A., Alasadi, A.A. and Faleh, N.M. (2019), "Nonlocal strain gradient thermal vibration analysis of double-coupled metal foam plate system with uniform and non-uniform porosities", *Coupl. Syst. Mech.*, **8**(3), 247-257. https://doi.org/10.12989/csm.2019.8.3.247.

Forsat, M., Badnava, S., Mirjavadi, S.S., Barati, M.R. and Hamouda, A.M.S. (2020), "Small scale effects on transient vibrations of porous FG cylindrical nanoshells based on nonlocal strain gradient theory", *Eur. Phys. J. Plus*, **135**(1), 81. https://doi.org/10.1140/epjp/s13360-019-00042-x.

Hadji, L., Zouatnia, N. and Bernard, F. (2019), "An analytical solution for bending and free vibration responses of functionally graded beams with porosities: Effect of the micromechanical models", *Struct. Eng. Mech.*, **69**(2), 231-241. https://doi.org/10.12989/sem.2019.69.2.231.

Hamad, L.B., Khalaf, B.S. and Faleh, N.M. (2019), "Analysis of static and dynamic characteristics of strain gradient shell structures made of porous nano-crystalline materials", *Adv. Mater. Res.*, **8**(3), 179. https://doi.org/10.12989/amr.2019.8.3.179.

Hamed, M.A., Mohamed, S.A. and Eltaher, M.A. (2020), "Buckling analysis of sandwich beam rested on elastic foundation and subjected to varying axial in-plane loads", *Steel Compos. Struct.*, **34**(1), 75-89. https://doi.org/10.12989/scs.2020.34.1.075.

Hamidi, A., Zidour, M., Bouakkaz, K. and Bensattalah, T. (2018), "Thermal and small-scale effects on vibration of embedded armchair single-walled carbon nanotubes", *J. Nano Res.*, **51**, 24-38. https://doi.org/10.4028/www.scientific.net/JNanoR.51.24.

Heshmati, M. and Jalali, S.K. (2019), "Effect of radially graded porosity on the free vibration behavior of circular and annular sandwich plates", *Eur. J. Mech.-A/Solid.*, **74**, 417-430. https://doi.org/10.1016/j.euromechsol.2018.12.009.

Iurlaro, L., Gherlone, M. and Di Sciuva, M. (2014), "Bending and free vibration analysis of functionally graded sandwich plates using the Refined Zigzag Theory", *J. Sandw. Struct. Mater.*, **16**(6), 669-699. https://doi.org/10.1177/1099636214548618.

Kant, T. and Swaminathan, K. (2002), "Analytical solutions for the static analysis of laminated composite and sandwich plates based on a higher order refined theory", *Compos. Struct.*, **56**(4), 329-344. https://doi.org/10.1016/s0263-8223(02)00017-x.

Kiani, Y. and Eslami, M.R. (2011), "Thermal buckling and post-buckling response of imperfect temperature-dependent sandwich FGM plates resting on elastic foundation", *Arch. Appl. Mech.*, **82**(7), 891-905. https://doi.org/10.1007/s00419-011-0599-8.

Li, Q., Iu, V.P. and Kou, K.P. (2008), "Three-dimensional vibration analysis of functionally graded material sandwich plates", *J. Sound Vib.*, **311**(1-2), 498-515. https://doi.org/10.1016/j.jsv.2007.09.018.

Lieu, Q.X., Lee, J., Lee, D., Lee, S., Kim, D. and Lee, J. (2018), "Shape and size optimization of functionally graded sandwich plates using isogeometric analysis and adaptive hybrid evolutionary firefly algorithm", *Thin Wall. Struct.*, **124**, 588-604. https://doi.org/10.1016/j.tws.2017.11.054.

Liu, N. and Jeffers, A.E. (2017), "Isogeometric analysis of laminated composite and functionally graded sandwich plates based on a layerwise displacement theory", *Compos. Struct.*, **176**, 143-153. https://doi.org/10.1016/j.compstruct.2017.05.037.

Mantari, J.L. and Granados, E.V. (2015), "A refined FSDT for the static analysis of functionally graded sandwich plates", *Thin Wall. Struct.*, **90**, 150-158. https://doi.org/10.1016/j.tws.2015.01.015.

Mantari, J.L., Oktem, A.S. and Guedes Soares, C. (2012), "A new trigonometric layerwise shear deformation theory for the finite element analysis of laminated composite and sandwich plates", *Comput. Struct.*, **94-95**, 45-53. https://doi.org/10.1016/j.compstruc.2011.12.003.

Mehar, K., Panda, S.K., Devarajan, Y. and Choubey, G. (2019), "Numerical buckling analysis of graded CNT-reinforced composite sandwich shell structure under thermal loading", *Compos. Struct.*, **216**, 406-414.

Mirjavadi, S.S., Forsat, M., Nikookar, M. Barati, M.R. and Hamouda, A.M.S. (2019b), "Nonlinear forced vibrations of sandwich smart nanobeams with two-phase piezo-magnetic face sheets", *Eur. Phys. J. Plus*, **134**, 508. https://doi.org/10.1140/epjp/i2019-12806-8.

Narwariya, M., Choudhury, A. and Sharma, A.K. (2018), "Harmonic analysis of moderately thick symmetric cross-ply laminated composite plate using FEM", *Adv. Comput. Des.*, **3**(2), 113-132. https://doi.org/10.12989/acd.2018.3.2.113.

Natarajan, S. and Manickam, G. (2012), "Bending and vibration of functionally graded material sandwich plates using an accurate theory", *Finite Elem. Anal. Des.*, **57**, 32-42. https://doi.org/10.1016/j.finel.2012.03.006.

Nayak, A.K., Moy, S.S.J. and Shenoi, R.A. (2002), "Free vibration analysis of composite sandwich plates based on Reddy's higher-order theory", *Compos. Part B: Eng.*, **33**(7), 505-519. https://doi.org/10.1016/s1359-8368(02)00035-5.

Nguyen, V.H., Nguyen, T.K., Thai, H.T. and Vo, T.P. (2014), "A new inverse trigonometric shear deformation theory for isotropic and functionally graded sandwich plates", *Compos. Part B: Eng.*, **66**, 233-246. https://doi.org/10.1016/j.compositesb.2014.05.012.

Othman, I.A.M. and Mahdy, A.S.M. (2018), "Numerical studies for solving a free convection boundary-layer flow over a vertical plate", *Mech. Mech. Eng.*, **22**(1), 35-42.

Othman, M.I.A., Abouelregal, A.E. and Said, S.M. (2019), "The effect of variable thermal conductivity on an infinite fiber-reinforced thick plate under initial stress", *J. Mech. Mater. Struct.*, **14**(2), 277-293. https://doi.org/10.2140/jomms.2019.14.277.

Pandey, S. and Pradyumna, S. (2015), "Free vibration of functionally graded sandwich plates in thermal environment using a layerwise theory", *Eur. J. Mech.-A/Solid.*, **51**, 55-66. https://doi.org/10.1016/j.euromechsol.2014.12.001.

Pandit, M.K., Sheikh, A.H. and Singh, B.N. (2008), "An improved higher order zigzag theory for the static analysis of laminated sandwich plate with soft core", *Finite Elem. Anal. Des.*, **44**(9-10), 602-610. https://doi.org/10.1016/j.finel.2008.02.001.

Panjehpour, M., Loh, E.W.K. and Deepak, T.J. (2018), "Structural insulated panels: State-of-the-art", *Trend. Civil Eng. Arch.*, **3**(1) 336-340.

Radwan, A.F. (2017), "Effects of non-linear hygrothermal conditions on the buckling of FG sandwich plates resting on elastic foundations using a hyperbolic shear deformation theory", *J. Sandw. Struct. Mater.*, **21**(1), 289-319. https://doi.org/10.1177/1099636217693557.

Raissi, H., Shishehsaz, M. and Moradi, S. (2018), "Stress distribution in a five-layer sandwich plate with FG face sheets using layerwise method", *Mech. Adv. Mater. Struct.*, 1-11. https://doi.org/10.1080/15376494.2018.1432796.

Rajabi, J. and Mohammadimehr, M. (2019), "Bending analysis of a micro sandwich skew plate using extended Kantorovich method based on Eshelby-Mori-Tanaka approach", *Comput. Concrete*, **23**(5), 361-376.

Rezaiee-Pajand, M., Arabi, E. and Masoodi, A.R. (2019), "Nonlinear analysis of FG-sandwich plates and shells", *Aerosp. Sci. Technol.*, **87**, 178-189. https://doi.org/10.1016/j.ast.2019.02.017.

Rezaiee-Pajand, M., Masoodi, A.R. and Mokhtari, M. (2018), "Static analysis of functionally graded non-prismatic sandwich beams", *Adv. Comput. Des.*, **3**(2), 165-190. https://doi.org/10.12989/acd.2018.3.2.165.

Safa, A., Hadji, L., Bourada, M. and Zouatnia, N. (2019), "Thermal vibration analysis of FGM beams using an efficient shear deformation beam theory", *Earthq. Struct.*, **17**(3), 329-336. https://doi.org/10.12989/eas.2019.17.3.329.

Sahouane, A., Hadji, L. and Bourada, M. (2019), "Numerical analysis for free vibration of functionally graded beams using an original HSDBT", *Earthq. Struct.*, **17**(1), 31-37. https://doi.org/10.12989/eas.2019.17.1.031.

Sedighi, H.M., Shirazi, K.H. and Attarzadeh, M.A. (2013), "A study on the quintic nonlinear beam vibrations using asymptotic approximate approaches", *Acta Astronautica*, **91**, 245-250. https://doi.org/10.1016/j.actaastro.2013.06.018.

Sedighi, H.M., Shirazi, K.H. and Zare, J. (2012a), "Novel equivalent function for deadzone nonlinearity: applied to analytical solution of beam vibration using He's Parameter Expanding Method", *Lat. Am. J. Solid. Struct.*, **9**(4), 443-452. https://doi.org/10.1590/s1679-78252012000400002.

Sedighi, H.M., Shirazi, K.H., Reza, A. and Zare, J. (2012b), "Accurate modeling of preload discontinuity in the analytical approach of the nonlinear free vibration of beams", *Proc. Inst. Mech. Eng., Part C: J. Mech. Eng. Sci.*, **226**(10), 2474-2484. https://doi.org/10.1177/0954406211435196.

Singh, S.J. and Harsha, S.P. (2018), "Exact solution for free vibration and buckling of sandwich S-FGM plates on pasternak elastic foundation with various boundary conditions", *Int. J. Struct. Stab. Dyn.*, **19**(3), 1950028. https://doi.org/10.1142/s0219455419500287.

Sobhy, M. (2013), "Buckling and free vibration of exponentially graded sandwich plates resting on elastic foundations under various boundary conditions", *Compos. Struct.*, **99**, 76-87. https://doi.org/10.1016/j.compstruct.2012.11.018.

Thai, C.H., Kulasegaram, S., Tran, L.V. and Nguyen-Xuan, H. (2014), "Generalized shear deformation theory for functionally graded isotropic and sandwich plates based on isogeometric approach", *Comput. Struct.*, **141**, 94-112. https://doi.org/10.1016/j.compstruc.2014.04.003.

Thai, H.T. and Kim, S.E. (2013), "Closed-form solution for buckling analysis of thick functionally graded plates on elastic foundation", *Int. J. Mech. Sci.*, **75**, 34-44. https://doi.org/10.1016/j.ijmecsci.2013.06.007.

Tomar, S.S. and Talha, M. (2018), "On the flexural and vibration behavior of imperfection sensitive higher order functionally graded material skew sandwich plates in thermal environment", *Proc. Inst. Mech. Eng., Part C: J. Mech. Eng. Sci.*, 095440621876695. https://doi.org/10.1177/0954406218766959.

Wang, B., Wu, L., Jin, X., Du, S., Sun, Y. and Ma, L. (2010), "Experimental investigation of 3D sandwich structure with core reinforced by composite columns", *Mater. Des.*, **31**(1), 158-165. https://doi.org/10.1016/j.matdes.2009.06.039.

Xiang, S., Jin, Y., Bi, Z., Jiang, S. and Yang, M. (2011), "A n-order shear deformation theory for free vibration of functionally graded and composite sandwich plates", *Compos. Struct.*, **93**(11), 2826-2832. https://doi.org/10.1016/j.compstruct.2011.05.022.

Yaghoobi, H. and Fereidoon, A. (2014), "Mechanical and thermal buckling analysis of functionally graded plates resting on elastic foundations: An assessment of a simple refined nth-order shear deformation theory", *Compos. Part B: Eng.*, **62**, 54-64. https://doi.org/10.1016/j.compositesb.2014.02.014.

Yaghoobi, H. and Torabi, M. (2013), "Exact solution for thermal buckling of functionally graded plates resting on elastic foundations with various boundary conditions", *J. Therm. Stress.*, **36**(9), 869-894. https://doi.org/10.1080/01495739.2013.770356.

Yazdani, R. and Mohammadimehr, M. (2019), "Double bonded Cooper-Naghdi micro sandwich cylindrical shells with porous core and CNTRC face sheets: Wave propagation solution", *Comput. Concrete*, **24**(6), 499-511.

Yeh, J.Y. (2013), "Vibration analysis of sandwich rectangular plates with magnetorheological elastomer damping treatment", *Smart Mater. Struct.*, **22**(3), 035010. https://doi.org/10.1088/0964-1726/22/3/035010.

Zenkour, A.M. and Sobhy, M. (2010), "Thermal buckling of various types of FGM sandwich plates", *Compos. Struct.*, **93**(1), 93-102. https://doi.org/10.1016/j.compstruct.2010.06.012.

Zenkour, A.M. and Sobhy, M. (2011), "Thermal buckling of functionally graded plates resting on elastic foundations using the trigonometric theory", *J. Therm. Stress.*, **34**(11), 1119-1138. https://doi.org/10.1080/01495739.2011.606017.

Zouatnia, N. and Hadji, L. (2019), "Effect of the micromechanical models on the bending of FGM beam using a new hyperbolic shear deformation theory", *Earthq. Struct.*, **16**(2), 177-183. https://doi.org/10.12989/eas.2019.16.2.177.

CC